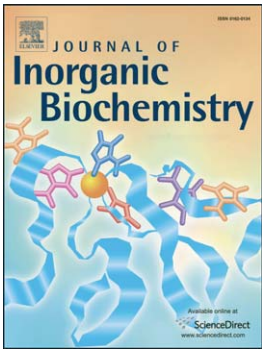

Anticancer Copper Pyridine Benzimidazole Complexes: ROS Generation, Biomolecule Interactions, and Cytotoxicity

Kathleen E. Prosser, Stephanie W. Chang, Felix Saraci, Phúc H. Lê, Charles J. Walsby

PII: S0162-0134(16)30377-4
DOI: doi:10.1016/j.jinorgbio.2016.11.006
Reference: JIB 10106

To appear in: *Journal of Inorganic Biochemistry*

Received date: 12 August 2016
Revised date: 12 October 2016
Accepted date: 3 November 2016

Please cite this article as: Kathleen E. Prosser, Stephanie W. Chang, Felix Saraci, Phúc H. Lê, Charles J. Walsby, Anticancer Copper Pyridine Benzimidazole Complexes: ROS Generation, Biomolecule Interactions, and Cytotoxicity, *Journal of Inorganic Biochemistry* (2016), doi:10.1016/j.jinorgbio.2016.11.006

Anticancer Copper Pyridine Benzimidazole Complexes: ROS Generation, Biomolecule Interactions, and Cytotoxicity

Kathleen E. Prosser, Stephanie W. Chang, Felix Saraci, Phúc H. Lê, and Charles J. Walsby*

Department of Chemistry, Simon Fraser University, 8888 University Dr, Burnaby, British Columbia, V5A 1S6, Canada

Keywords: copper; anticancer; reactive oxygen species; albumin; DNA

***Corresponding Author.**
Email address: cwalsby@sfu.ca
TEL: 778-782-4607
FAX: 778-782-3765

ABSTRACT: The Cu(II) complex $CuCl_2$(pbzH), pbzH = 2-(2-pyridinyl)benzimidazole, and derivatives modified at the non-coordinated nitrogen of the benzimidazole fragment, have been studied as anticancer agents. These compounds show promising cytotoxicity against A549 adenocarcinomic alveolar basal epithelial cells with IC_{50} values in the range of 5-10 μM. Importantly, this activity is higher than either $CuCl_2 \cdot H_2O$ or the individual ligands, demonstrating that ligand coordination to the Cu(II) centres of the complexes is required for full activity. Electron paramagnetic resonance (EPR) and UV-Vis spectroscopies were used to characterize the solution behaviour of the complexes. These studies demonstrate: (i) two types of solvated species in buffer, (ii) both coordinate and non-coordinate interactions with albumin, and (iii) weak interactions with DNA. Further DNA studies using agarose gel electrophoresis demonstrate strand cleavage by the complexes in the presence of ascorbate, which is mediated by reactive oxygen species (ROS). Through a fluorescence-based *in vitro* assay, intracellular ROS generation in the A549 cell line was observed; indicating that damage by ROS is responsible for the observed activity of the complexes.

INTRODUCTION

Copper-based chemotherapeutics[1-4] are attracting increasing interest as alternatives to non-essential metal-based drugs, such as those containing platinum,[5] ruthenium,[6, 7] and gold.[8] Copper is an endogenous metal that is vital to the function of all organisms,[9] but is highly toxic if not properly trafficked.[10] Toxicity originates primarily from damage to biological macromolecules through redox-reactions, especially via formation of reactive oxygen species (ROS).[11] The Cu(II)/Cu(I) redox-couple is the major source of these reactions and is influenced by the ligand environment of copper centres.[12]

Reports of copper chemotherapeutics are dominated by complexes of the 2+ oxidation state, primarily due to the diversity of structures afforded to this oxidation state derived from diverse donor atoms (N, O, S and halides), coordination numbers (four to six), and geometries.[1-4, 13] An array of copper compounds has been evaluated using both *in vitro* testing and *in vivo* animal studies.[1, 2] Antitumor activity from Cu complexes with diverse ligand systems, including thiosemicarbazones, mixed chelates, tetradentate ligands, and Schiff bases, have been reported *in vivo*.[1, 2] To date, none of these complexes have progressed to human clinical trials as chemotherapeutics in their own right. However, copper gluconate coadministered with the dithiocarbamate compound disulfiram is currently under clinical development for the treatment of solid liver tumors,[14] and glioblastomas.[15-17] In this case, anticancer activity may involve generation of a bis(*N*,*N*-diethyl dithiocarbamato)copper(II) complex and induction of oxidative stress.[18, 19]

Cu complexes with bidentate N-N donors derived from heterocyclic ring systems have been widely reported, in many cases showing promising anticancer activity. Notable ligand types include phenanthroline and bipyridine derivatives, pyrazole-pyridine ligands, and benzimidazole

based ligands.[1, 3] The origin of the anticancer activity of these types of Cu complexes has been linked to DNA interactions, enzyme inhibition, and redox-mediated generation of ROS.[3]

The ligands used in the work described herein are based on 2-(2-pyridinyl)benzimidazole (pbzH) (**Scheme 1**), which inhibits hepatic enzymes,[20] and exhibits antiplasmodial[21] and anticancer[22] activities. The synthesis of Cu(II)(pbzH)Cl_2 has been described,[23, 24] but the complex has not previously been studied for medicinal properties. However, the anticancer activity of metal-pbzH complexes has been explored using ruthenium,[25] gold,[26] palladium, and platinum.[27-29] Furthermore, several bis-pbzH Cu(II) complexes have been structurally characterized,[30-32] with one such compound demonstrating *in vitro* anticancer activity.[33] A number of related mixed-ligand complexes with other ancillary ligands have also been structurally characterized and examined for their DNA cleaving abilities and for antibacterial activity.[34-36] These studies suggest the viability of these types of complexes for use in a therapeutic setting.

In this study, we have synthesized and characterized Cu(pbzH)Cl_2 and five derivatives with functionalization at the non-coordinated pbz benzimidazole nitrogen (**Scheme 1**). This study is a rare example of a chemical and biological investigation of copper complexes that have both labile coordination sites and N,N-donor ligands.[1, 2, 13, 37] We describe a variety of approaches to characterize these Cu(II) complexes and their biological behaviour, including electron paramagnetic resonance (EPR) spectroscopy, electrochemistry, DNA gel electrophoresis, and *in vitro* assays, providing insight into their cytotoxic activity. Overall, these studies demonstrate that Cu(II)(pbzH)Cl_2 is a promising chemotherapeutic scaffold, with well-defined biological interactions and activity derived from the redox-active copper center.

RESULTS AND DISCUSSION

1. Synthesis and structures

The synthetic method used for the ligands pbzX (**Scheme 1**) is based on the literature report of Huang *et al.*,[38, 39] which gives the compounds in reasonable yields under mild conditions. One particularly appealing feature of these ligands from a medicinal perspective is that they can be functionalized readily. As we demonstrate here, modification at the non-coordinated nitrogen of the benzimidazole fragment potentially enables inclusion of a variety of functional groups. The Cu(pbzX) complexes were synthesized as shown in **Scheme 1**, based on literature reports for the synthesis of dichloro copper benzimidazole compounds.[37] The pure copper complexes can be isolated without residual solvent following trituration with ether. The identity and purity of all compounds was confirmed by elemental analysis, IR spectroscopy, mass spectrometry, and X-ray crystallography where possible.

X-ray crystal structures for complexes Cu(pbzBz), Cu(pbzF), Cu($pbzF_2$) and Cu($pbzF_5$) were determined, shown in **Figure 1**. In each case, crystals suitable for X-ray analysis were obtained from concentrated acetonitrile solutions at low temperature. However, despite attempts under a range of conditions, Cu(pbzH) and Cu(pbzMe) could only be obtained as fine powders, indicating that the benzyl groups of the other complexes play an important role in promoting crystallization.

Each of the crystal structures demonstrates bidentate coordination of the pbzX ligands through the nitrogens of the benzimidazole and pyridyl moieties. The structures of Cu(pbzF) and Cu($pbzF_5$) show mononuclear complexes with distorted square-planar geometries around the Cu(II) centers. In the case of Cu(pbzBz) and Cu($pbzF_2$), dimeric structures are observed with the individual Cu(II) centers exhibiting distorted trigonal bipyramidal geometries, and two chloride

ligands providing a μ^2 bridge between them. The dichloro bridge contains two distinct bond lengths of 2.26 and 2.68 Å for Cu(pbzBz) and 2.26 and 2.76 Å for Cu(pbzF_2) (see **Table S2** for all Cu centered bond lengths). These observations are similar to the Cu(II) phenanthroline (phen) dimer [CuCl(phen)μ-Cl]$_2$, where the μ^2-chloro bridge has two shorter Cu-Cl bonds (2.26 Å) and longer Cu-Cl bonds (2.68 Å),[40] indicating that this is common structural feature in these types of complexes. Given the asymmetry in the Cu-Cl bonds linking the Cu centers of Cu(pbzBz) and Cu(pbzF_2), the dimeric structures observed are assigned to a consequence of crystal packing forces, with monomeric Cu(II) centres similar to Cu(pbzF) and Cu(pbzF_5) expected once the solid is dissolved in solution. This is demonstrated by EPR measurements (see below) where the spectra of all of the complexes are similar and typical for mononuclear S = 1/2 Cu(II) complexes, with no evidence for exchange coupling between Cu centres for Cu(pbzBz) and Cu(pbzF_2).[41]

2. Anticancer Activity

The *in vitro* anticancer activity of compounds Cu(pbzX) was assessed against A549 adenocarcinomic alveolar basal epithelial cells, a non-small cell lung cancer (NSCLC) cell line. In the clinic, NSCLC is often treated with cisplatin, and has a 5-year survival rate that is below 50%.[42, 43] In addition to testing the Cu(pbzX) complexes, cisplatin, and each of the six pbzX ligands were also tested as controls for activity. Furthermore, $CuCl_2 \cdot 2H_2O$ was also tested, as a model for the activity of free copper.

All of the compounds were incubated with A549 cells for 72 hours to assess their cytotoxic effect at concentrations ranging from 0.625 to 100 μM. In these experiments, all wells contained 1% dimethyl sulfoxide (DMSO), which was also tested as the vehicle control. This concentration of DMSO is tolerated by A549 cells and allows for sufficient solubility of all

compounds tested. The solubility of the complexes was assessed at all concentrations by checking for precipitation by examination under a microscope and during plate imaging. Furthermore, UV-Vis spectra at 50 μM concentrations also showed no evidence of precipitation. The fraction of cells affected in each case was imaged using a fluorescent cell-permeable nuclear marker (Hoescht 33342 nucleic acid stain) to determine the total cell count, and a cell impermeable nuclear marker (ethidium homodimer I) to count the number of dead cells. Statistical analysis of the resulting images gave sigmoidal dose-response curves (**Figure 2**) that were modelled using a four-parameter logistic model to calculate the 50% inhibitory concentration (IC_{50}) values (**Table 1**).

Each of the Cu(pbzX) complexes demonstrated strong cytotoxic activity with IC_{50} values ranging from 5.5 to 12 μM. This compares favourably with cisplatin, which had an IC_{50} value of 3.5 μM against the A549 cell line (**Figure S24**). Cu(pbzMe) was the most active complex, with activity that was the same as cisplatin at the $p < 0.001$ level of significance. The activity of $CuCl_2 \cdot 2H_2O$ was significantly lower ($p < 0.001$) than any of the Cu(pbzX) complexes with an IC_{50} value of 32 μM. Similarly, all of the pbzX ligands showed only moderate to low cytotoxicity. The most active ligand $pbzF_2$ had IC_{50} = 30 μM and three of the ligands, pbzH, pbzMe and $pbzF_5$, did not achieve 50% inhibition of cell growth at the highest tested concentrations of 100 μM. The low level of activity of the ligands may be due in part to low solubility in aqueous media or DMSO, although under the assay conditions no significant precipitation was observed under a microscope or during image analysis. Importantly, there is no correlation between the activity of the ligands and the corresponding Cu(II) complexes. Indeed, two of the ligands with the lowest responses (pbzH and pbzMe) give the most active complexes. Taken together, these data highlight the necessity of both the copper centre and the pbzX ligands

for the observed cytotoxic activity. When compared to other copper complexes tested against A549 cells, the Cu(pbzX) complexes perform as well as or better than most. A few examples include a Cu-quercetin complex with an IC_{50} of 21.5 μM,[44] a set of binuclear complexes with an average IC_{50} of 10 μM[45] and copper complexes with nitroimidazole[46] and N, N, N donors [47] having average IC_{50} values of 15 and 67 μM, respectively.

3. Electrochemical Properties.

Cyclic voltammograms from solutions of each complex in 2-(*N*-morpholino)ethanesulfonic acid (MES) buffer were collected (**Figure S22**) to probe the effect of the ligands pbzX on the reduction potentials of the complexes, and the impact of ligand exchange processes. A scan rate of 25 mV/s was chosen for these experiments due to slow electron transfer rates which have been reported for similar Cu complexes.[48] Cyclic voltammograms were measured at pH 4.4 since at higher pH (pH 6.5, 7.4 for example) significant peak broadening and irreversibility was observed, likely due to formation of insoluble copper hydroxide species.[49] Even at pH 4.4 all of the complexes exhibited relatively broad peaks, likely due to overlapping waves from different species arising from ligand exchange in solution. This was particularly evident for Cu(pbzH) and Cu(pbzMe), which showed wide peaks and evidence for irreversibility. By contrast, the benzyl substituted complexes give rise to narrower and more reversible waves, likely reflecting greater solution stability at pH 4.4 The $E°'$ values of the complexes (**Table 1**) range from 295 mV for Cu(pbzMe) to 370 mV for Cu($pbzF_5$). These reduction potentials are within a typical range for copper compounds with aromatic nitrogen-containing ligands.[50] There is a trend of increasing reduction potentials with the addition of fluorines to the pendant benzene ring ($E°'$: Cu(pbzBz) < Cu(pbzF) < Cu($pbzF_2$) < Cu($pbzF_5$)) which can be attributed to the electron-withdrawing effects of the fluorine substituents. Similarly, the electron donating methyl group of Cu(pbzMe) results

in the lowest reduction potential.

The principal motivation for characterizing the electrochemistry in aqueous solutions was to evaluate whether the Cu(II)/Cu(I) couples were within the range of common biological reductants. Based on reduction potentials for Cu(pbzX), in the range of 295-370 mV, all of these complexes could undergo reduction by biological reducing agents such as glutathione ($E°'$ = –240 mV)[51] or ascorbate ($E°'$ = –50 mV).[52] Thus, we conclude that the complexes will be reduced in the *in vitro* experiments described below. This demonstrates the relevance of the gel electrophoresis studies of DNA cleavage that implicate hydroxyl radical generation as the source of cytotoxic activity. Furthermore, this is consistent with the observation of the generation of ROS by Cu(pbzX) in A549 cells (see below).

4. Solution Behaviour.

Ligand exchange processes are central to the activity of many metal-based chemotherapeutics since they determine the pharmacologically important species *in vivo*. Consequently, anticancer metallodrugs such as platinum[53] and ruthenium[54] complexes are considered to be pro-drugs that exchange ligands to generate activated species. Following administration, the original ligands of such complexes can by replaced by water and other prevalent small molecules, as well as biomolecules such as DNA and proteins.[54, 55] In the case of copper complexes, such as those described here, ligand exchange is highly favoured under physiological conditions,[56] and so characterization of these processes is required to understand their mechanisms. We have applied EPR and UV-Vis spectroscopies to define changes to the coordination environment of the Cu(pbzX) complexes.

EPR analysis. The paramagnetic Cu(II) centers (d^9, S = ½) of the Cu(pbzX) complexes enabled

EPR studies of their solution behavior and interactions with biomolecules. Spectra were analysed using the MATLAB program EasySpin[57] to determine g values and hyperfine interactions with the copper centers of the complexes (^{63}Cu, 69.17%, I = 3/2, g_N = +1.4824; ^{65}Cu, 30.83%, I = 3/2, g_N = +1.5878) and nitrogen nuclei (^{14}N, I = 1, 99.63%) of the ligands. Simulations of Cu hyperfine splittings include appropriately weighted contributions from both isotopes, and scaled values of copper hyperfine interactions according to $A(^{63}Cu)/A(^{65}Cu) = g_N(^{63}Cu)/g_N(^{65}Cu)$; values of A(Cu) are quoted for the more abundant ^{63}Cu isotope. For solutions containing multiple Cu(II) species, spectra from individual species were identified and their respective simulated spectra added together with appropriate weightings to reproduce the experimental data. EPR measurements of Cu(pbzX) in frozen solutions showed uniaxial spectra (with one exception, see below) with $g_\parallel > g_\perp$. This is consistent with Cu(II) ions in square planar or axially elongated octahedral crystal fields, with the unpaired electron in the $d_{x^2-y^2}$ orbital, indicating that this is the approximate geometry of the Cu(II) species generated from Cu(pbzX) in solution. To first-order in perturbation theory, the g values are given by $g_\parallel = 2 - \frac{8\lambda}{\Delta_1}$ and $g_\perp = 2 - \frac{2\lambda}{\Delta_2}$, where the spin- orbit coupling coefficient (λ) is estimated to be 85% that of the free ion (free Cu(II) ion: –828 cm^{-1}, here: –700 cm^{-1}) and Δ_1 is the energy difference between $d_{x^2-y^2}$ and the d_{xy}, orbitals and Δ_2 is the energy difference between $d_{x^2-y^2}$ and the degenerate d_{xz} and d_{yz} orbitals.[58]

Complexes in MES buffer. The EPR spectra of the complexes in MES buffer (pH 6.5) show contributions from two Cu(II) species (**Figure 3**, **Figures S17-18**). With the exception of Cu(pbzH), the Cu(pbzX) complexes showed similar spectra with both species having uniaxial g tensors: MES-1 ($g_\perp$ = 2.064-2.065, $g_\parallel$ = 2.256-2.258), MES-2 ($g_\perp$ = 2.069-2.070, $g_\parallel$ = 2.315-2.320). Both species also exhibit copper hyperfine interactions around $g_\parallel$: MES-1 ($A_\parallel$ (Cu) = 185-190 G), MES-2 ($A_\parallel$ (Cu) = 170-172 G). Complex Cu(pbzH) also shows the uniaxial spectrum

from species MES-2 detected from the other complexes. However, a uniaxial spectrum corresponding to MES-1 was not observed from Cu(pbzH), but instead a rhombic spectrum with g = [2.247, 2.100, 1.925] and A_1 = 200 MHz was detected (**Figures S17-18, Table S3**). This is likely due to the exchangeable proton of the benzimidazole of the pbzH ligand, which is otherwise functionalized in the other complexes. Deprotonation of the ligand would result in generation of an effective negative charge on the benzimidazole ring, perturbing the ligand field of the Cu centre and leading to a loss of degeneracy of the d_{xz} and d_{yz} orbitals, resulting in splitting of $g_\perp$ into two distinct g values. Spectral deconvolution of each of the complexes determined that MES-2 was the predominant species, comprising around 2/3 of the total spectral intensity in each case.

By taking numerical derivatives of the EPR spectra, to give second-derivative line shapes, additional hyperfine structure was resolved in the $g_\perp$ region of each complex (**Figure 3b**, **Figure S18**). This was simulated by including copper hyperfine coupling ($A_\perp$(Cu) = 2-9 G) and hyperfine interactions from two nitrogen nuclei with approximately equal coupling constants ($A_\perp(^{14}N)$ = 14-15 G) in the simulation of MES-2. Spectral overlap in the $g_\perp$ region meant that resolution of such splittings from the secondary species MES-1 was not possible. Nonetheless, observation of hyperfine structure from two nitrogen atoms is consistent with coordinated pbzX ligands.

The EPR spectra on their own do not enable unequivocal assignment of the species present when Cu(pbzX) are dissolved in MES buffer. However, the rapid ligand-exchange rates of Cu(II) complexes[56] suggests that the chloride ligands will be replaced by water ligands in aqueous solution. Furthermore, comparison of the EPR spectra with previous studies of Cu(II) phenanthroline in aqueous solution are instructive. Indeed, the EPR spectra of the substituted

Cu(pbzX) complexes are remarkably similar to those reported for $[Cu(phen)]^{2+}$ in aqueous solution,[59] which shows two species with $g_{\|}$ = 2.314, $A_{\|}$ (Cu) = 179 G and $g_{\|}$ = 2.259, $A_{\|}$ (Cu) = 184 G. In this earlier study, these species were identified as the di-aquo complex and its deprotonated aquo-hydroxy derivative respectively. Based on the striking similarities in spectral parameters we provisionally assign MES-1 as $[Cu(pbzX)(OH_2)(OH)]^{+}$ and MES-2 as $[Cu(pbzX)(OH_2)_2]^{2+}$. This implies that exchange of both Cl^{-} ligands from Cu(pbzX) is completed in the course of preparing the EPR samples; attempts to minimize ligand exchange by freezing samples immediately after mixing with the buffer solution did not change the appearance of the spectra. In the case of the unsubstituted complex Cu(pbzH), deprotonation of $[Cu(pbzH)(OH_2)_2]^{2+}$ (MES-2) at the ligand, rather than coordinated water, to give $[Cu(pbz)(OH_2)_2]^{+}$ is consistent with the observation of a species with a rhombic EPR spectrum, rather than the uniaxial MES-1 signal observed with the other complexes.

UV-Vis spectra of the Cu(pbzX) complexes in MES buffer show a strong absorbance at ~320 nm from a ligand centered transition. Time dependent UV-Vis spectra (**Figure S13**) of each complex show little change over the course of one hour at 37 °C. This is again consistent with chloride ligand exchange occurring on a time scale faster than sample preparation. Due to limited aqueous solubility, it was not possible to monitor the more diagnostic Cu(II) d-d absorption bands at longer wavelengths.

5. Interactions with Human Serum Albumin.

Serum proteins, such as human serum albumin (HSA), have been implicated in the transport and bioaccumulation of many inorganic anticancer agents.[60] HSA binds Cu(II) with high affinity, with the primary binding site located at the *N*-terminus involving coordination by histidine, two

peptide nitrogens, and the terminal aspartic acid α-NH_2.[61, 62] HSA has several exposed surface histidines, as well as hydrophobic binding sites, each of which have been implicated in the transport of medicinal metal complexes.[63-66]

To establish whether HSA could be a transporter of Cu(pbzX), the complexes were incubated with the protein, and protein-bound fractions were isolated by ultrafiltration. The EPR spectra of each complex with HSA show the presence of two species (**Figure 4**, and **Figure S19**). The first of these species, HSA-1, has g values ($g_\perp$ = 2.033-2.043, $g_\parallel$ = 2.180-2.189) that are distinct from either of the species in MES buffer. Furthermore, the copper hyperfine interaction of HSA-1 ($A_\parallel$ (Cu) = 207-215 G) is significantly larger than either of the buffer species. The hyperfine splitting pattern around $g_\perp$ of HSA-1 is comprised of unique contributions from both nitrogen and copper interactions, which are partially resolved in the experimental EPR data and well defined in the second-derivative spectra (**Figure 4b**, and **Figure S20**). Simulations demonstrate that the hyperfine structure is derived from contributions of both the copper centre ($A_\perp$(65Cu) = 17-18 G) and three approximately equivalent nitrogens ($A(^{14}N)$ = 14.5 G.) The relatively large value of $A_\perp$(65Cu), as compared to MES-1, further demonstrates that HSA-1 is distinct from either of the species in MES buffer. However, even more significant is the observation of contributions from three nitrogens. Since only two coordinated nitrogens are provided by the pbzX ligands, this demonstrates an additional nitrogen atom coordinated to the copper centre that arises from HSA. This species is likely from coordination to the imidazole side-chains of histidines.

The second species observed in the presence of HSA, HSA-2, has g values and copper hyperfine couplings ($g_\perp$ = 2.052-2.063, $g_\parallel$ = 2.267-2.295, $A_\parallel$ (Cu) = 180-185 G) that are similar to MES-2. This suggests that a fraction of the complexes are not coordinated to the protein.

However, since the samples studied are isolated protein-bound fractions, this may reflect non-coordinate interactions with HSA, as has been reported for a variety of metal complexes, particularly with hydrophobic sites.[65-69] Small differences in g values and hyperfine couplings may be ascribed to the influence of second coordination sphere effects.[70] Interestingly, while Cu(pbzH) shows a rhombic spectrum in MES, the complex shows a uniaxial spectrum with similar parameters to the other complexes with HSA. This suggests that the uncoordinated benzimidazole is protonated in the presence of the HSA, and may reflect the effect of the local environment in the protein. Overall, the EPR data show that the Cu(pbzX) complexes readily form both coordinate and non-coordinate interactions with HSA. This is promising since such interactions are associated with metallodrug transport to tumour sites *in vivo*, and could provide a route for bioaccumulation.[71]

6. Interactions with DNA

The ability to intercalate or cleave DNA has been linked to the activity of several Cu-based anticancer agents.[72-77] To determine if this behaviour was involved in the cytotoxicity of Cu(pbzX), the interactions of the complexes with calf-thymus DNA (ctDNA) and bacterial plasmid DNA were characterized using UV-Vis titrations, EPR measurements, and gel electrophoresis.

UV-Vis titrations. The reaction of the Cu(pbzX) complexes with ctDNA was characterized by concentration-dependent changes in the absorption spectrum. To quantify the DNA interactions of Cu(pbzX), each complex (50 μM) was incubated with ctDNA (50 - 350 μM molar base-pair concentration) for 40 minutes. Titrating the complexes with increasing concentrations of DNA resulted a red shift and hypochromism of the λ_{max} (**Figure S14**), changes which are indicative of

intercalation. This has been shown, for example, in studies of Cu(II) phenanthroline complexes.[78] These data were analyzed for each complex using **Equation 1** to calculate binding constants K_b:[79]

$$\frac{[\text{DNA}]}{(\varepsilon_A - \varepsilon_f)} = \frac{[\text{DNA}]}{\varepsilon_B - \varepsilon_f} + \frac{1}{K_b(\varepsilon_B - \varepsilon_f)} \quad (1)$$

where [DNA] is the molar concentration of base pairs, ε_B is the extinction coefficient of the complex fully bound to DNA, ε_A is the apparent extinction coefficient of the complex bound to DNA and ε_f is the extinction coefficient of the complex free in solution. A plot of [DNA] vs. [DNA]/($\varepsilon_A - \varepsilon_f$) gives a linear relationship with K_b calculated by dividing the slope by the intercept. Such plots for each Cu(pbzX) complex are shown in **Figure S15**, with corresponding values of K_b in **Table 1**. Overall, the magnitude of the binding constants for all of the complexes (10^4 M^{-1}) is well below that of classic intercalators, which typically have K_b values in the 10^{5-6} M^{-1} range.[80] These relatively low binding constant agree with the results from gel electrophoresis studies (see below) where significant intercalation was also not observed, and demonstrate that while there is an interaction between the Cu(pbzX) complexes and DNA, it is unlikely to be by a strong intercalative mechanism.

EPR. To further characterize interactions between Cu(pbzX) and DNA, EPR spectra were collected from each complex with ctDNA in MES buffer (**Figure S21** and **Table S5**). The resulting spectra show two distinct species with uniaxial EPR signals: DNA-1 ($g_\perp$ = 2.055-2.076, $g_\parallel$ = 2.326-2.330, $A_\parallel$ (Cu) = 154-160 G), DNA-2 ($g_\perp$ = 2.057-2.064, $g_\parallel$ = 2.285-2.287, $A_\parallel$ (Cu) = 167-170 G). The g values of these species are close to those of the uniaxial spectra from the buffer species MES-1 and MES-2, respectively, indicating a similar primary coordination sphere in each case. However, the differences in the g values although small are still significant, as

determined from the spectral simulations, particularly for $g_{\|}$. This is assigned to secondary coordination sphere effects,[70] resulting from interaction with DNA.

The uniaxial species DNA-1 and DNA-2, when compared to MES-1 and MES-2, have values of $A_{\|}$ (Cu) that are reduced by 12-15 and 16-22 G, respectively. This observation, and the changes in g values, are similar to literature reports of $[Cu(phen)(H_2O)_3]^{2+}$ interacting with DNA.[59] Using DNA-fiber EPR, it has been shown that these signals from the phenanthroline complex are assignable to a combination of intercalative and minor-groove binding.[81] Based on the UV-Vis studies described above, the Cu(pbzX) complexes only weakly intercalate with ctDNA, thus the EPR signals are more likely to reflect groove binding.

Additional evidence for DNA interactions is provided by the EPR spectrum from Cu(pbzH) (**Figure S21a**). In this case a contribution from the rhombic species previously observed from the MES buffer sample (MES-2) is observed in addition to the uniaxial signals DNA-1 and DNA-2. Based on relative signal intensities determined by simulation, this indicates ~1/3 of Cu(pbzH) is found in solution, rather than interacting with DNA, which is consistent with weak binding.

Gel Electrophoresis and ROS effects. To further examine interactions with DNA, electrophoresis experiments using agarose gels and pet22b plasmid DNA were performed. Plasmids are a useful tool for these studies because they are found primarily in three forms that migrate at different rates on the gel. From fastest to slowest these forms are: i) supercoiled (SC), ii) linear (L), which is the result of a double-strand break, and iii) open circular (OC), which is seen as a consequence of single-strand breaks or nicks.[82] In addition, intercalation between base pairs, or kinking of the strands, can induce changes to the migration rate of SC plasmids.[83, 84] SC is the naturally occurring form of plasmid DNA and is therefore the most prominent band.

However, the process through which the plasmids were isolated in this work resulted in small amounts of the L and OC forms in all samples.

The Cu(pbzX) complexes were first incubated with plasmid DNA only. As shown in **Figure 5a,** this did not result in any change to the rate of migration or the relative concentration of the three DNA forms, as compared to the control. Thus, we conclude that the Cu complexes alone do not substantially intercalate or otherwise modify the DNA. To explore ROS generation as the origin of anticancer activity, the Cu(pbzX) complexes were incubated with plasmid DNA and sodium ascorbate. Addition of ascorbate generates Cu(I) species, which can be concluded from the reduction potentials of the complexes (see above), and these can initiate Fenton-like chemistry to produce ROS.[85, 86] The combined action of the complexes and ascorbate is evident in **Figure 5b**, where there is a clear transformation of the plasmids from the SC to the L form. This transformation indicates a double-strand cleavage of the DNA through an oxidative damage pathway involving ROS.[87, 88] These experiments were repeated with each of the pbzX ligands alone (**Figure S23**), which showed no change from the control. This is consistent with the cleavage process being driven by the copper centres of the complexes.

To probe the DNA-cleavage mechanism, superoxide dismutase (SOD) and catalase were used as enzymatic scavengers of superoxide and peroxide respectively. Incubation of the Cu(pbzX) complexes with plasmid DNA, sodium ascorbate, and 1 unit of SOD (**Figure 5c**) gave results that were indistinguishable from experiments without the enzyme. For every complex there was still a clear transformation of the SC for of the plasmid to the L form. However, incubation of the plasmids with sodium ascorbate, 1 Unit of catalase, and each of the Cu(pbzX) complexes, inhibited DNA cleavage (**Figure 5d**), demonstrating that hydrogen peroxide is important to the DNA cleavage process.

We propose the step-wise mechanism of ROS generation shown in **Scheme 2**. Initial reduction of Cu(pbzX) by ascorbate enables generation of superoxide from molecular oxygen.[89] The reduced form of Cu(pbzX) then catalyzes reduction of superoxide to hydrogen peroxide. In our gel experiments, it is following this step that catalase inhibited further catalysis to the active species. In the absence of catalase, H_2O_2 is further reduced to give a hydroxyl radical and hydroxide.[89] Incubation with SOD fails to inhibit DNA cleavage because SOD catalyzes the reduction of superoxide to hydrogen peroxide,[90, 91] which ultimately promotes the formation of hydroxyl radicals (**Scheme 2**). While hydroxyl radicals were not directly detected in these experiments, previous studies of Cu(II) complexes with reducing agents have established hydrogen peroxide as an intermediate step in their generation, as well as their role in cleaving DNA.[87, 92, 93]

7. *In Vitro* ROS Measurements

Fluorescence-based assays of ROS generated by the Cu(pbzX) complexes with A549 cells were performed using the non-polar cell-permeable dye, 2,7-dichlorodihydrofluorescein diacetate (DCFH-DA).[94-97] This non-fluorescent molecule readily diffuses across cell membranes, after which its acetate groups are enzymatically hydrolyzed by intracellular esterases to give 2,7-dichlorodihydrofluorescein (DCFH).[95, 97] Oxidation of DCFH produces 2,7-dichlorofluorescein (DCF), which is fluorescent due to its extended π system, enabling quantification of ROS species *in vitro*. The A549 cells were exposed to the Cu(pbzX) complexes and imaged after 1.5 hours of incubation. The fluorescence of each sample was normalized to a media control, with positive controls provided by 1 and 10 μM H_2O_2, and statistical significance was assessed using Student's t test. The results of this assay are summarized in **Figure 6**.

All of the complexes produce elevated levels of ROS versus the media control, with at

least as much ROS activity as the 1 μM H_2O_2 positive control. While DCFH is a well-established probe for cellular peroxides, H_2O_2 alone does not directly oxidize DCFH.[97, 98] By contrast, hydroxyl radicals do readily oxidize DCFH, so that detection of H_2O_2 requires decomposition into radicals.[97, 98] This may occur either by Fenton chemistry in the presence of reduced metal ions such as Cu(I) or Fe(II), or by cellular peroxidases.[99] Additionally, it has been reported that superoxide is not capable of oxidizing DCFH.[97, 99] Thus, the observation of DCFH oxidation when the cells are exposed to Cu(pbzX) is consistent with the mechanism determined in the DNA electrophoresis studies (see above). In the cell studies, endogenous reducing agents likely reduce the Cu(pbzX) complexes to Cu(I) species, initiating a redox cascade analogous to that in **Scheme 2**, where molecular oxygen is reduced to H_2O_2 and ultimately converted to hydroxyl radicals.

Cu(pbzMe) showed the greatest increase in ROS, reaching the same level as the 10 μM H_2O_2 positive control. Interestingly, this complex also has highest cytotoxic activity against A549 cells (see above), further implicating ROS in the mechanism of action of these types of complexes. Overall, the observation of elevated ROS in the A549 cells in the presence of Cu(pbzX) is further evidence for a mechanism of action involving oxidative DNA damage.

CONCLUSIONS

The ongoing development of copper complexes as potential chemotherapeutics is dependent on characterization of active species and mechanisms of anticancer activity. In this study we have used a variety of physical and biological methods to characterize the Cu(pbzX) complexes. These compounds are useful models for the medicinal application of copper complexes with chelating nitrogen donors and exchangeable ligands. The latter are less common features of

reported Cu anticancer candidates, but as we show here, they can play an important role in biological speciation. Another feature of the pbz ligands is functionalization at the non-coordinated nitrogen of the benzimidazole moiety, which provides a mode for modification of their properties. This suggests that these complexes could be a useful scaffold for development of multifunctional Cu(II) metallotherapeutics.

The Cu(pbzX) complexes are comprised of three components that influence their pharmacological behaviour: exchangeable chlorides, a non-exchangeable hydrophobic pbzX ligand, and a redox-active Cu(II) centre. As we show here, each one of these components plays a key role in the cytotoxicity and pharmacological behaviour of the compounds.

From EPR and UV-Vis studies we have shown that the chloride ligands are likely rapidly exchanged under physiological conditions to give aquo- and hydroxo-coordinated species. Thus, Cu(pbzX) complexes can be considered to be potential pro-drugs. An important consequence of the ligand-exchange processes of metallodrug candidates is coordination to biomolecules. In the case of the Cu(pbzX) complexes, EPR spectra demonstrate coordination to HSA, likely though a histidine imidazole. Analysis of the nitrogen hyperfine structure from these species shows that this process leaves the pbzX ligands coordinated, and introduces an additional nitrogen-donor ligand from the protein.

The hydrophobic non-exchangeable pbzX ligands also influence interactions with biomolecules. This is shown by a second type of EPR signal from the Cu(pbzX) complexes in the presence of HSA, that is similar, though distinct from, species observed in buffer. Since isolated protein fractions were characterized in these studies, these signals indicate non-coordinate interactions with HSA, possibly with hydrophobic binding domains. This observation, and detection of HSA-coordinated species, indicates that if complexes of this type were

administered intravenously that they would be found significantly associated with HSA. By contrast, EPR measurements and UV-Vis titrations indicate that the pbzX ligands mediate only relatively weak interactions with DNA. These techniques show respectively that new species are formed upon incubation with DNA and that one possible mode of interaction is weak intercalation.

The central role that the copper centres of the Cu(pbzX) complexes play in their anticancer activity is shown by the electrochemical, gel electrophoresis, and *in vitro* studies reported here. The reduction potentials of all of the complexes are within the range of biological reducing agents. Generation of Cu(I) species and redox cycling can then lead to generation of ROS. As we show by gel studies with ascorbate and SOD or catalase, hydroxide radicals are likely the ultimate result of this process. The relevance of these results to the mechanism of anticancer activity is shown by detection of elevated ROS levels in A549 cells in the presence of Cu(pbzX). Notably, the compound with the highest activity, Cu(pbzMe), also generates the highest level of ROS *in vitro*.

Perhaps the most important observation in this work is that the cytotoxicity of the Cu(pbzX) complexes is greater than either the pbzX ligands on their own or free Cu(II). This may indicate that the ligands play a role in enabling the copper centres to effectively generate elevated levels of toxic ROS, leading to cell death. We suggest that this could be the result of enhanced transport into cells, subsequent intracellular targeting, or perhaps a consequence of altered chemical properties such as modulated reduction potentials. Work is currently being undertaken to further examine the enhanced biological activity of Cu(pbzX) complexes over copper chloride and the implications for the rational design of new Cu(II) anticancer agents.

EXPERIMENTAL

Synthesis. The starting compounds $CuCl_2 \cdot 2H_2O$, o-phenylenediamine, 2-picolinic acid, iodomethane, benzyl bromide (Fisher Scientific), 4-fluorobenzyl bromide, 3,5-fluorobenzyl bromide and pentafluorobenzyl bromide (Sigma-Aldrich) were used without further purification. All of the ligands pbzX were prepared according to the general procedures reported by Huang *et al.* for 2-(2-pyridinyl)benzimidazole (pbzH), 1-methyl-2-(2-pyridinyl)benzimidazole (pbzMe), and 1-(phenylmethyl)-2-(2-pyridinyl)benzimidazole (pbzBz).[38, 39] Syntheses of 1-[(4-fluorphenyl)methyl)-2-(2-pyridinyl)benzimidazole (pbzF)[100] and 1-[(2,3,4,5,6-pentafluorphenyl)methyl)-2-(2-pyridinyl)benzimidazole ($pbzF_5$)[101] have also been reported using other methods, whereas 1-[(3, 5-difluorphenyl)methyl)-2-(2-pyridinyl)benzimidazole ($pbzF_2$) is, to our knowledge, a new compound. The synthetic procedure is outlined in **Scheme 1**, where in the first step pbzH was produced by the reaction of 2-picolinic acid and o-phenalinediamine in polyphosphoric acid (PPA). The derivatized ligands were then produced by reaction of pbzH in a dimethylformamide (DMF) solution of $K_2CO_3$with either iodomethane to give pbzMe, or with the appropriate benzyl bromide to give pbzBz, pbzF, $pbzF_2$, and $pbzF_5$. Details of synthetic methods and ^{1}H NMR (**Figures S1-6**) are provided in Supporting Information.

All Cu complexes were synthesized using the same general procedure, based on the literature synthesis of dichloro copper benzimidazole complexes,[37] and outlined in **Scheme 1**. The pbzX ligands (0.5 mmol) were dissolved in minimal DMF and added to a solution of $CuCl_2 \cdot 2H_2O$ (8.5 mg, 0.5 mmol) dissolved in 0.5 mL of DMF. The combined solutions were stirred at room temperature, during which time a precipitate formed. The complexes were isolated via suction filtration and thoroughly dried under reduced pressure. Structure and purity were verified using

elemental analyses, Fourier transform infrared spectroscopy (FT-IR) (**Figures S7-12**), X-ray crystallography and matrix-assisted laser desorption/ionization - time of flight (MALDI-TOF) mass spectrometry. Detailed physical characterization and synthetic procedures for each complex can be found in the Supporting Information.

Crystallographic Structure Determination. Single crystal X-ray diffraction analysis was performed on a Bruker SMART diffractometer equipped with an APEX II CCD area detector, a Mo Kα fine focus sealed tube (λ = 0.71073 nm) and a Cu Kα fine focus sealed tube (λ = 1.54178 nm) operating at 1.5 kW (50 kV, 30 mA), and filtered with a graphite monochromator. The temperature was regulated using an Oxford Cryosystems Cryostream to 150 K when necessary. The structures were solved by direct methods, and subsequent refinements were performed using SHELXL and shelXle. For Cu(pbzBz), reflections (-4 0 8, 0 0 6, 1 1 5, 1 2 4, 2 2 2) were omitted due to systematic error. Structure diagrams were generated by ORTEP-3(v. 2.00) and rendered using Adobe Illustrator (CS6). Crystal data, data collection parameters, and details of structure refinement are listed in **Table S1**. CCDC-1496889-1496892 contains the supplementary crystallographic data for this paper. These data can be obtained free of charge from The Cambridge Crystallographic Data Centre via www.ccdc.cam.ac.uk/data%5Frequest/cif.

Electrochemical Measurements. Stock solutions (10 mM) of each compound were initially prepared in DMSO to improve solubility in aqueous media. Cyclic voltammograms were recorded on a CH Instruments 660 potentiostat, equipped with a Ag/AgCl (1 M KCl) reference electrode, a platinum wire counter electrode and a basal plane graphite working electrode. The basal plane graphite electrode was prepared using a modified literature preparation using electrochemically inert Loctite 9460 Hysol Epoxy to seal the carbon blocks.[102] All data were collected in an aqueous buffer solution at pH 4.4 consisting of 10 mM 2-(N-

morpholino)ethanesulfonic acid (MES) and 150 mM NaCl. $K_3[Fe(CN)_6]$ was used to calibrate the electrode potential. Measurements were performed using 150 µM concentrations of each complex with final concentrations of 1.5% DMSO in 3 mL of MES buffer using a 25 mV/s scan rate.

Cell Studies. A549 cells were acquired directly from Dr. Marcel Bally's lab (Vancouver, BC) at the British Columbia Cancer Research Agency. Cells were cultured at 37 °C under a 5% CO_2 atmosphere in RPMI 1640 media (Gibco) supplemented with 2 mM L-glutamine (Gibco) and 10% fetal bovine serum (Gibco). All of the Cu compounds were diluted from 10 mM stocks in DMSO to give the desired concentrations in complete cellular media for cytotoxicity testing. To verify that the compounds would remain soluble under assay conditions, each compound was incubated in complete cell media at the maximum testing concentrations for 72 hours at 37 °C and in each case there was no evidence of precipitation.

For *in vitro* cytotoxicity assays, cells were seeded in quadruplet at 2000 cells/well in 384-well plates (Greiner Bio-One). Following a 24 hr incubation period, 20 µL aliquots of each complex in media were added to each well to give the desired complex concentration with a final DMSO content of 1%. Wells containing a media control and a vehicle (DMSO) control also were prepared. The cells were stained using 5 µL of a 10 mg/mL stock of Hoescht 33342 nucleic acid stain (Life Technologies) and 3 µL of a 1 mM stock of ethidium homodimer I (Biotium) per mL of media. These stains were added 72 hrs after treatment by each complex, generating a total cell count and a dead cell count respectively. After a 20-minute incubation period the plates were then imaged using an IN Cell Analyzer 1000 (GE Healthcare), which is an automated fluorescent microscopy platform that enables high content screening. Cell counts were determined via the IN Cell Developer Toolbox software. Cells were classified as "dead" if they showed >30% overlap

of the two stains. Statistical analyses to determine IC_{50} were performed using GraphPad software.

For *in vitro* ROS assays, cells were seeded at 50,000 cells/well in a 96-well plate (Grener Bio-One). Following a 24 hr incubation period, the culture medium was aspirated off and 100 µL of 10 µM 2′,7′-dichlorofluorescin diacetate (Sigma Aldrich) in sterile phosphate buffered saline (PBS) was added to each well and subsequently incubated for 45 minutes. The PBS was removed via aspiration and fresh media with 10 µM of the respective Cu complexes was added to each well. Wells containing 1 and 10 µM H_2O_2 were used as positive controls to establish concentration dependence. After 1.5 hours the plates were imaged using the IN Cell Analyzer 1000 with five images and 10× magnification. Cell counts were then determined via the IN Cell Developer Toolbox software. Due to scatter in the data associated with incomplete well coverage by the images, outliers were eliminated before calculation of the average number of fluorescent cells and statistical significance was determined by Student's t-test.

DNA electrophoresis gels. Plasmid DNA (pet22b, Novagen, 5493bp) was isolated and purified using a Qiagen MaxiPrep Kit. A 20 µM stock solution of plasmid in water was used as the starting material for all successive solutions. Stock solutions of each ligand and copper complex in DMSO (10 mM) were prepared to facilitate solubility in aqueous media. Fresh stock solutions (8 µM) of each ligand and complex were prepared in 10 mM MES buffer, with 150 mM NaCl, immediately prior to sample preparation. Using these aqueous stock solutions, all samples consisted of 10 µM DNA and 2 µM ligand or copper complex. In addition, buffer, sodium ascorbate (20 µM), superoxide dismutase (SOD) (10 Units), and/or catalase (1 Unit) were added to the appropriate samples such that the final volume was 20 µL.

Samples were incubated at 37 °C for 30 min, after which time the reactions were quenched with 2.2 µL of a 10× loading buffer containing 50% (v/v) glycerol, 100 mM $Na_2EDTA•2H_2O$ (EDTA = ethylenediaminetetraacetic acid), 1% (v/v) sodium dodecyl sulfate and 0.1% bromophenol blue (v/v) in deionized water. Samples were then stored at −4 °C until immediately prior to loading onto agarose gel. Electrophoresis was performed on an agarose gel (0.8%) in a Life Technologies Horizon 58 apparatus for 60 min at 90 V in 1X tris-acetate-EDTA buffer. The completed gels were incubated for 45 min in a 5 µg/mL solution of ethidium bromide, washed for in distilled water, and imaged under UV light.

UV-Vis Experiments. Measurements were conducted on a Cary 100 Bio UV-Visible spectrophotometer with a water temperature controlled thermostat 6×6 Multicell Block Peltier cooling module. Prior to the preparation of the final samples, stock solutions of each compound were prepared in DMSO to enhance solubility in aqueous media. All spectra were collected at 37 °C.

Complexes in Buffer. To 746.25 µL of MES buffer (pH 6.5) was added 3.75 µL of the 10 mM stock solution of each complex in DMSO to give 50 µM solutions of each compound. UV-Vis spectra were collected every 5 min over the course of one hour.

DNA Titrations. Calf-thymus DNA (ctDNA, Invitrogen, Thermo Fisher Scientific) was supplied as 10 mg/mL solutions. A series of solutions were prepared from DMSO stock solutions of the copper complexes (5 mM) to give samples containing copper complex (50 µM) and ctDNA (0 µM, 50 µM, 150 µM, 250 µM, 350 µM). $Cu(pbzF_2)$ required the preparation of a 100 µM sample because the absorbance of the 350 µM significantly overlapped with that of the ctDNA

and could not be determined. Samples were incubated for 40 min at 37 °C and the absorption spectrum collected.

EPR Measurements and Simulations. EPR spectra were collected at X-band (9.3−9.4 GHz) using a Bruker EMXplus spectrometer with a PremiumX microwave bridge and HS resonator. Using a Bruker ER 4112HV helium temperature-control system and continuous-flow cryostat with liquid nitrogen, spectra were collect at 100 K. To facilitate the comparison of samples, the concentration of complexes and spectroscopic parameters were unchanged for each experiment. A quartz-insert tube holder, which is a part of the Bruker cryostat system, ensures reproducible sample placement within the EPR resonator. Automatic tuning of the spectrometer gave a Q-factor of 6500 ± 10%, indicating limited variation in instrument sensitivity.

Preparations of EPR Samples. For all samples, 10 mM stock solutions of each compound were prepared in DMSO, to facilitate subsequent dissolution in aqueous buffered solutions.

Complexes in Buffer. A 500 µM solution of each complex was prepared in MES buffer pH 6.5 using the DMSO stocks. Aliquots of 210 µL were promptly mixed with 90 µL of glycerol, and immediately frozen in liquid nitrogen.

Complexes with human serum albumin. A 600 µL solution of 250 µM HSA with 500 µM of each complex was prepared in MES buffer. These solutions were diluted to a final volume of 4 mL then incubated for one hour at 37 °C. Following incubation, samples were concentrated down to a volume of 200 µL using an Amicon centrifugal filter unit (30 kDa molecular-weight cutoff) by centrifuging at 4500 rpm for 30 min at 4 °C. The filtered product was collected and mixed with 90 µL of glycerol and 10 µL of MES buffer to give a final volume of 300 µL. Samples were then transferred to EPR tubes and frozen in liquid nitrogen.

Complexes with ctDNA. A 210 µL solution containing 500 µM of each complex in MES buffer, and 2 mM of ctDNA, was incubated for one hour at 37 °C. These solutions were then mixed with 90 µL of glycerol, transferred to EPR tubes, and frozen in liquid nitrogen.

ABBREVIATIONS

ctDNA	Calf-thymus DNA
DCF	Dichlorofluorescein
DCFH	Dichlorodihydrofluorescein
DCFH-DA	2′,7′-dichlorofluorescin diacetate
DMF	Dimethylformamide
DMSO	Dimethyl sulfoxide
EDTA	Ethylenediaminetetraacetic acid
EPR	Electron paramagnetic resonance
FT-IR	Fourier transform infrared spectroscopy
HSA	Human serum albumin
IC_{50}	Inhibitory concentration 50%
L	Linear
MALDI-TOF	Matrix-assisted laser desorption/ionization - time of flight
MES	2-(*N*-morpholino)ethanesulfonic acid
NSCLC	Non-small cell lung cancer
OC	Open circular
pbzBz	1-(phenylmethyl)-2-(2-pyridinyl)benzimidazole
pbzF	1-[(4-fluorphenyl)methyl)-2-(2-pyridinyl)benzimidazole
$pbzF_2$	1-[(3, 5-difluorphenyl)methyl)-2-(2-pyridinyl)benzimidazole
$pbzF_5$	1-[(2,3,4,5,6-pentafluorphenyl)methyl)-2-(2-pyridinyl)benzimidazole
pbzH	2-(2-pyridinyl)benzimidazole
pbzMe	1-methyl-2-(2-pyridinyl)benzimidazole
phen	Phenanthroline
PPA	Polyphosphoric acid
ROS	Reactive oxygen species
SC	Supercoiled
SOD	Superoxide dismutase

ACKNOWLEDGEMENTS

Financial support was provided by The Natural Sciences and Engineering Research Council of Canada (NSERC) and Simon Fraser University (SFU). K.E.P. acknowledges additional support

from NSERC through a Vanier Canada Graduate Scholarship. P.H.L. acknowledges support from Mitacs Canada through a Globalink Research Award. The authors are extremely grateful to Marcel Bally at the BC Cancer Research Agency (Vancouver, BC, Canada) for providing the A549 cells, and for access to tissue culture and cell imaging facilities. The authors also wish to thank Robert Young (SFU) for access to GraphPad software, and Jeffrey Warren (SFU) for use of electrochemical facilities.

REFERENCES

[1] C. Marzano, M. Pellei, F. Tisato, C. Santini, Anticancer Agents Med. Chem. 2009, 9, 185-211.

[2] C. Santini, M. Pellei, V. Gandin, M. Porchia, F. Tisato, C. Marzano, Chem. Rev. 2014, 114, 815-862.

[3] S. Tardito, L. Marchiò, Curr. Med. Chem. 2009, 16, 1325-1348.

[4] F. Tisato, C. Marzano, M. Porchia, M. Pellei, C. Santini, Med. Res. Rev. 2010, 30, 708-749.

[5] I. Ali, W. A. Wani, K. Saleem, A. Haque, Anticancer Agents Med. Chem. 2013, 13, 296-306.

[6] A. Bergamo, G. Sava, Dalton Trans. 2011, 40, 7817-7823.

[7] I. Kostova, Curr. Med. Chem. 2006, 13, 1085-1107.

[8] T. Zou, C. T. Lum, C.-N. Lok, J.-J. Zhang, C.-M. Che, Chem. Soc. Rev. 2015.

[9] W. Mertz, Science 1981, 213, 1332-1338.

[10] L. M. Gaetke, C. K. Chow, Toxicology 2003, 189, 147-163.

[11] B. Halliwell, J. M. C. Gutteridge, in Methods in Enzymology, Vol. 86 (Eds.: L. Packer, A. N. Glazer), Academic Press, 1990, pp. 1-85.

[12] N. Kitajima, Y. Moro-oka, Chem. Rev. 1994, 94, 737-757.

[13] C. Duncan, A. R. White, Metallomics 2012, 4, 127-138.

[14] H. C. I. University of Utah, https://clinicaltrials.gov/ct2/show/NCT00742911, 2014.

[15] S. Sahlgrenska University Hospital, ClinicalTrials.gov, 2016.

[16] W. U. S. o. Medicine, clinicaltrials.gov, 2016.

[17] O. M. Center, clinicaltrials.gov, 2017.

[18] D. J. Lewis, P. Deshmukh, A. A. Tedstone, F. Tuna, P. O'Brien, Chem. Commun. 2014, 50, 13334-13337.

[19] C. N. Hancock, L. H. Stockwin, B. Han, R. D. Divelbiss, J. H. Jun, S. V. Malhotra, M. G. Hollingshead, D. L. Newton, Free Radic. Biol. Med. 2011, 50, 110-121.

[20] M. Murray, A. J. Ryan, P. J. Little, J. Med. Chem. 1982, 25, 887-892.

[21] Z. S. Saify, M. K. Azim, W. Ahmad, M. Nisa, D. E. Goldberg, S. A. Hussain, S. Akhtar, A. Akram, A. Arayne, A. Oksman, I. A. Khan, Bioorg. Med. Chem. Lett. 2012, 22, 1282-1286.

[22] V. A. Sontakke, S. Ghosh, P. P. Lawande, B. A. Chopade, V. S. Shinde, ISRN Org. Chem. 2013, 2013, 453682.

[23] B. Chiswell, F. Lions, B. S. Morris, Inorg. Chem. 1964, 3, 110-114.

[24] T. J. Lane, I. Nakagawa, J. L. Walter, A. J. Kandathil, Inorg. Chem. 1962, 1, 267-276.

[25] M. Martínez-Alonso, N. Busto, F. A. Jalón, B. R. Manzano, J. M. Leal, A. M. Rodríguez, B. García, G. Espino, Inorg. Chem. 2014, 53, 11274-11288.

[26] L. Maiore, M. C. Aragoni, C. Deiana, M. A. Cinellu, F. Isaia, V. Lippolis, A. Pintus, M. Serratrice, M. Arca, Inorg. Chem. 2014, 53, 4068-4080.

[27] G. Tallen, C. Mock, S. B. Gangopadhyay, B. Kangarloo, B. Krebs, J. E. Wolff, Anticancer Res. 2000, 20, 445-449.

[28] C. Mock, I. Puscasu, M. J. Rauterkus, G. Tallen, J. E. A. Wolff, B. Krebs, Inorg. Chim. Acta. 2001, 319, 109-116.

[29] J. S. Casas, A. Castiñeiras, E. García-Martínez, Y. Parajó, M. L. Pérez-Parallé, A. Sánchez-González, J. Sordo, Z. Anorg. Allg. Chem. 2005, 631, 2258-2264.

[30] M. Altaf, H. Stoeckli-Evans, Transition Met Chem 2009, 34, 613-620.

[31] B. Machura, A. Świtlicka, M. Wolff, J. Kusz, R. Kruszynski, Polyhedron 2009, 28, 1348-1354.

[32] E. Spodine, A. Atria, P. Meza, Transition Met Chem 1986, 11, 205-207.

[33] A. S. a. Technology, J. Inorg. Biochem. 2007, 101, 881-892.

[34] D. Choquesillo-Lazarte, B. Covelo, J. M. González-Pérez, A. Castiñeiras, J. Niclós-Gutiérrez, Polyhedron 2002, 21, 1485-1495.

[35] X.-B. Fu, Z.-H. Lin, H.-F. Liu, X.-Y. Le, Spectrochim. Acta, Part A 2014, 122, 22-33.

[36] Z. B. Ou, Y. H. Lu, Y. M. Lu, S. Chen, Y. H. Xiong, X. H. Zhou, Z. W. Mao, X. Y. Le, J. Coord. Chem. 2013, 66, 2152-2165.

[37] F. Sączewski, E. Dziemidowicz-Borys, P. J. Bednarski, R. Grünert, M. Gdaniec, P. Tabin, J. Inorg. Biochem. 2006, 100, 1389-1398.

[38] W.-K. Huang, C.-W. Cheng, S.-M. Chang, Y.-P. Lee, E. W.-G. Diau, Chem. Commun. 2010, 46, 8992-8994.

[39] W.-K. Huang, H.-P. Wu, P.-L. Lin, Y.-P. Lee, E. W.-G. Diau, J. Phys. Chem. Lett. 2012, 3, 1830-1835.

[40] M. Mroueh, C. Daher, E. Hariri, S. Demirdjian, S. Isber, E. S. Choi, B. Mirtamizdoust, H. H. Hammud, Chem. Biol. Interact. 2015, 231, 53-60.

[41] C. Chow, R. D. Willett, J. Chem. Phys. 1973, 59, 5903-5915.

[42] D. C. Chan, K. A. Earle, T. L. M. Zhao, B. Helfrich, C. Zeng, A. Baron, C. M. Whitehead, G. Piazza, R. Pamukcu, W. J. Thompson, H. Alila, P. Nelson, P. A. Bunn, Clin. Cancer Res. 2002, 8, 904-912.

[43] J. Zhang, T. Zhang, X. Ti, J. Shi, C. Wu, X. Ren, H. Yin, Biochem. Biophys. Res. Commun. 2010, 399, 1-6.

[44] J. Tan, B. Wang, L. Zhu, JBIC, J. Biol. Inorg. Chem. 2009, 14, 727-739.

[45] X.-W. Li, X. Li, Y.-T. Li, Z.-Y. Wu, C.-W. Yan, J. Organomet. Chem. 2012, 700, 48-57.

[46] M. Pellei, G. Papini, A. Trasatti, M. Giorgetti, D. Tonelli, M. Minicucci, C. Marzano, V. Gandin, G. Aquilanti, A. Dolmella, C. Santini, Dalton Trans. 2011, 40, 9877-9888.

[47] P. Kumar, S. Gorai, M. Kumar Santra, B. Mondal, D. Manna, Dalton Trans. 2012, 41, 7573-7581.

[48] B. Xie, T. Elder, L. J. Wilson, D. M. Stanbury, Inorg. Chem. 1999, 38, 12-19.

[49] P. Haack, C. Limberg, Angew. Chem. Int. Ed. 2014, 53, 4282-4293.

[50] P. Majumdar, A. K. Ghosh, L. R. Falvello, S.-M. Peng, S. Goswami, Inorg. Chem. 1998, 37, 1651-1654.

[51] J. Rost, S. Rapoport, Nature 1964, 201, 185-185.

[52] C. Creutz, Inorg. Chem. 1981, 20, 4449-4452.

[53] T. C. Johnstone, K. Suntharalingam, S. J. Lippard, Chem. Phys. Lett 2016, 116, 3436-3486.

[54] E. Reisner, V. B. Arion, B. K. Keppler, A. J. L. Pombeiro, Inorg. Chim. Acta. 2008, 361, 1569-1583.

[55] G. Chu, J. Biol. Chem. 1994, 269, 787-790.

[56] L. Helm, A. E. Merbach, Chem. Rev. 2005, 105, 1923-1959.

[57] S. Stoll, A. Schweiger, J. Magn. Reson. 2006, 178, 42-55.

[58] J. R. Pilbrow, Transition Ion Electron Paramagnetic Resonance, Clarendon Press, 1990.

[59] M. Chikira, Y. Tomizawa, D. Fukita, T. Sugizaki, N. Sugawara, T. Yamazaki, A. Sasano, H. Shindo, M. Palaniandavar, W. E. Antholine, J. Inorg. Biochem. 2002, 89, 163-173.

[60] A. R. Timerbaev, C. G. Hartinger, S. S. Aleksenko, B. K. Keppler, Chem. Rev. 2006, 106, 2224-2248.

[61] A. G. Bearn, H. G. Kunkel, Proc. Soc. Exp. Biol. Med. 1954, 85, 44-48.

[62] M. Valko, H. Morris, M. Mazur, J. Telser, E. J. L. McInnes, F. E. Mabbs, J. Phys. Chem. B 1999, 103, 5591-5597.

[63] F. Kratz, VCH, 1993, pp. 391-429.

[64] B. P. Esposito, R. Najjar, Coord. Chem. Rev. 2002, 232, 137-149.

[65] O. Doemoetoer, C. G. Hartinger, A. K. Bytzek, T. Kiss, B. K. Keppler, E. A. Enyedy, JBIC, J. Biol. Inorg. Chem. 2013, 18, 9-17.

[66] S. W. Chang, A. R. Lewis, K. E. Prosser, J. R. Thompson, M. Gladkikh, M. B. Bally, J. J. Warren, C. J. Walsby, Inorg. Chem. 2016, 55, 4850-4863.

[67] S. Tabassum, W. M. Al-Asbahy, M. Afzal, F. Arjmand, J. Photochem. Photobiol., B 2012, 114, 132-139.

[68] A. D. Tinoco, E. V. Eames, C. D. Incarvito, A. M. Valentine, Inorg. Chem. 2008, 47, 8380-8390.

[69] L. Yan, X. Wang, Y. Wang, Y. Zhang, Y. Li, Z. Guo, J. Inorg. Biochem. 2012, 106, 46-51.

[70] M. L. Souza, E. E. Castellano, J. Telser, D. W. Franco, Inorg. Chem. 2015, 54, 2067-2080.

[71] N. Cetinbas, M. Webb, J. Dubland, C. Walsby, JBIC, J. Biol. Inorg. Chem. 2010, 15, 131-145.

[72] X. Qiao, Z.-Y. Ma, J. Shao, W.-G. Bao, J.-Y. Xu, Z.-Y. Qiang, J.-S. Lou, BioMetals 2014, 27, 155-172.

[73] V. Rajendiran, R. Karthik, M. Palaniandavar, V. S. Periasamy, M. A. Akbarsha, B. S. Srinag, H. Krishnamurthy, Inorg. Chem. 2007, 46, 8208-8221.

[74] S. Ramakrishnan, V. Rajendiran, M. Palaniandavar, V. S. Periasamy, B. S. Srinag, H. Krishnamurthy, M. A. Akbarsha, Inorg. Chem. 2009, 48, 1309-1322.

[75] S. Zhang, Y. Zhu, C. Tu, H. Wei, Z. Yang, L. Lin, J. Ding, J. Zhang, Z. Guo, J. Inorg. Biochem. 2004, 98, 2099-2106.

[76] P. U. Maheswari, S. Roy, H. den Dulk, S. Barends, G. van Wezel, B. Kozlevčar, P. Gamez, J. Reedijk, J. Am. Chem. Soc. 2006, 128, 710-711.

[77] F. V. Pamatong, C. A. Detmer, J. R. Bocarsly, J. Am. Chem. Soc. 1996, 118, 5339-5345.

[78] Z. Yang, Y. Wang, G. Yang, BioMetals 2011, 24, 737-745.

[79] A. Wolfe, G. H. Shimer, T. Meehan, Biochemistry 1987, 26, 6392-6396.

[80] J.-B. LePecq, C. Paoletti, J. Mol. Biol. 1967, 27, 87-106.

[81] M. Chikira, C. H. Ng, M. Palaniandavar, Int. J. Mol. Sci. 2015, 16, 22754-22780.

[82] P. H. Johnson, L. I. Grossman, Biochemistry 1977, 16, 4217-4225.

[83] M. V. Keck, S. J. Lippard, J. Am. Chem. Soc. 1992, 114, 3386-3390.

[84] O. Novakova, H. Chen, O. Vrana, A. Rodger, P. J. Sadler, V. Brabec, Biochemistry 2003, 42, 11544-11554.

[85] A. N. Pham, G. Xing, C. J. Miller, T. D. Waite, J. Catal. 2013, 301, 54-64.

[86] M. Valko, C. J. Rhodes, J. Moncol, M. Izakovic, M. Mazur, Chem. Biol. Interact. 2006, 160, 1-40.

[87] J. A. Imlay, S. Linn, Science 1988, 240, 1302-1309.

[88] E. S. Henle, S. Linn, J. Biol. Chem. 1997, 272, 19095-19098.

[89] A. N. Pham, A. L. Rose, T. D. Waite, J. Phys. Chem. A 2012, 116, 6590-6599.

[90] I. Fridovich, Science 1978, 201, 875-880.

[91] D. Jourd'heuil, F. S. Laroux, D. Kang, A. M. Miles, D. A. Wink, M. B. Grisham, Methods Enzymol. 1999, 301, 220-227.

[92] B. G. Que, K. M. Downey, A. G. So, Biochemistry 1980, 19, 5987-5991.

[93] D. S. Sigman, D. R. Graham, V. D'Aurora, A. M. Stern, J. Biol. Chem. 1979, 254, 12269-12272.

[94] A. S. Keston, R. Brandt, Anal. Biochem. 1965, 11, 1-5.

[95] A. Gomes, E. Fernandes, J. L. F. C. Lima, J. Biochem. Biophys. Methods 2005, 65, 45-80.

[96] H. Wang, J. A. Joseph, Free Radic. Biol. Med. 1999, 27, 612-616.

[97] B. Halliwell, M. Whiteman, Br. J. Pharmacol. 2004, 142, 231-255.

[98] O. Myhre, J. M. Andersen, H. Aarnes, F. Fonnum, Biochem. Pharmacol. 2003, 65, 1575-1582.

[99] C. P. LeBel, H. Ischiropoulos, S. C. Bondy, Chem. Res. Toxicol. 1992, 5, 227-231.

[100] O. Celik, F. Angay, M. Gundogan, M. Ulusoy, Acta Crystallogr., Sect. E: Struct. Rep. Online 2014, 70, o485.

[101] N. M. Shavaleev, Z. R. Bell, T. L. Easun, R. Rutkaite, L. Swanson, M. D. Ward, Dalton Trans. 2004, 3678-3688.

[102] J. D. Blakemore, N. D. Schley, D. Balcells, J. F. Hull, G. W. Olack, C. D. Incarvito, O. Eisenstein, G. W. Brudvig, R. H. Crabtree, J. Am. Chem. Soc. 2010, 132, 16017-16029.

TABLES, FIGURE/SCHEME CAPTIONS, AND FIGURES

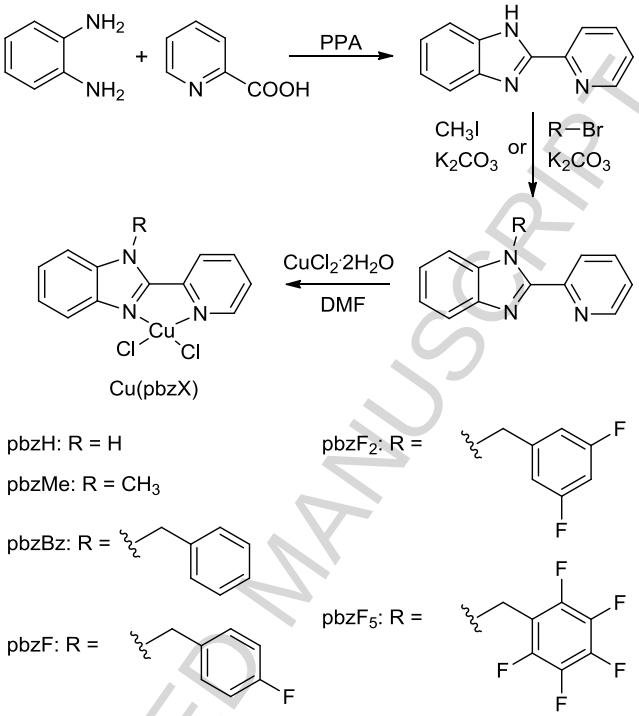

Scheme 1. Reaction scheme for the synthesis of each of the ligands (pbzX) and of their corresponding copper complexes (Cu(pbzX)).

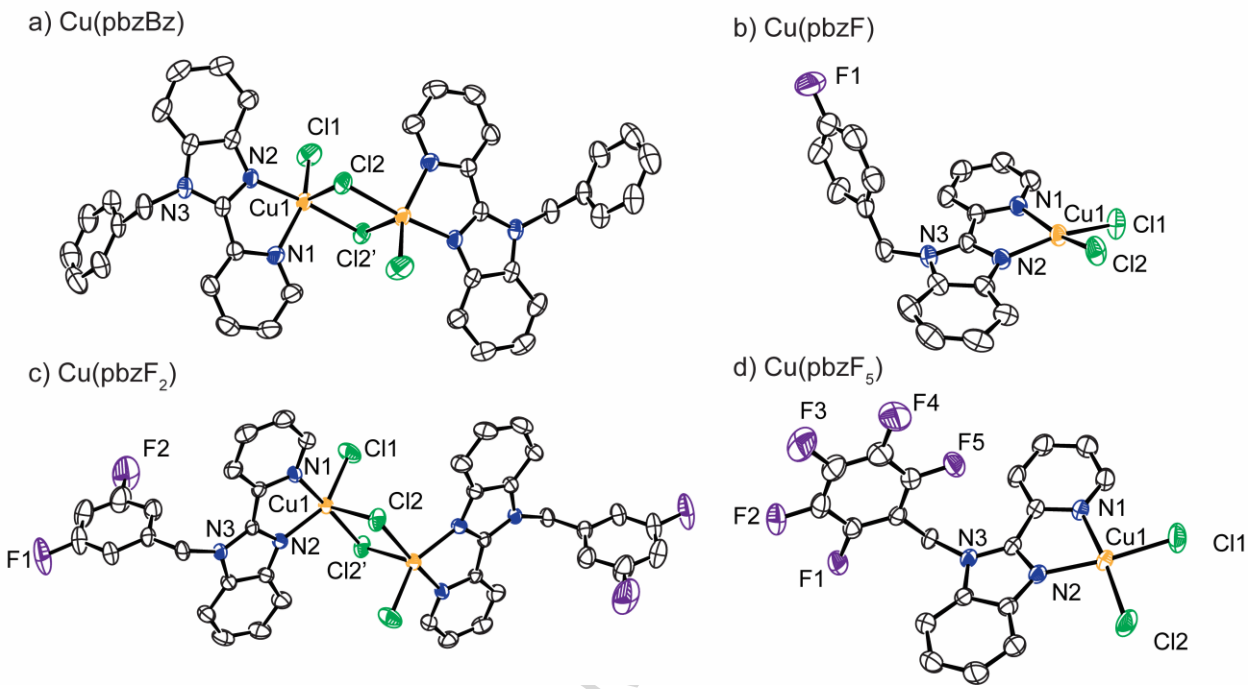

Figure 1. Crystal structures of: a) Cu(pbzBz), b) Cu(pbzF), c) Cu(pbzF_2), and d) Cu(pbzF_5). Thermal ellipsoids drawn at the 50% probability level.

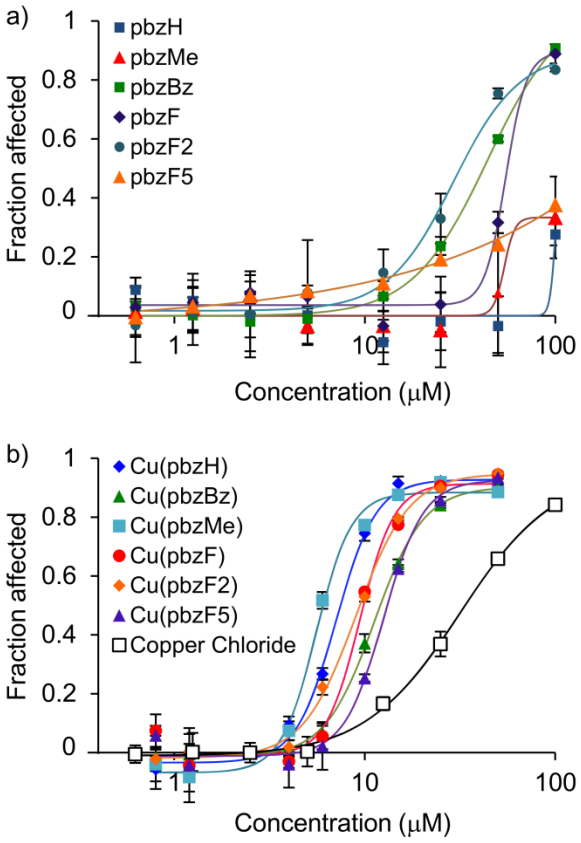

Figure 2. Dose-response curves against the A549 non-small cell lung cancer cell line. Sigmoidal curves were fitted to the data using GraphPad statistical analysis software. Shown are a) the six pbzX ligands and b) the six Cu(pbzX) complexes and $CuCl_2 \cdot 2H_2O$.

Table 1. IC_{50} values of all tested compounds against the A549 non-small cell lung cancer cell line, as determined by fitting to a four parameter logistic model to collected fraction affected data. DNA binding constants determined based on absorbance titration measurements. $E^{\circ\prime}$ as determined by cyclic voltammetry in MES buffer at pH 4.4.

	IC_{50} Ligand (μM)	IC_{50} Cu Complex (μM)[a]	Complex DNA K_b (10^4 M^{-1})	Complex $E^{\circ\prime}$ (mV vs. NHE, ± 5)
pbzH	>100	7 ± 0.3	2.5 ± 0.9	~ 330
pbzMe	>100	5.5 ± 0.4	1.5 ± 0.7	295
pbzBz	50 ± 10	11.2 ± 0.4	1.4 ± 0.8	320
pbzF	70 ± 40	9.4 ± 0.5	5 ± 3	325
$pbzF_2$	30 ± 8	9.0 ± 0.9	1.4 ± 0.6	335
$pbzF_5$	>100	12 ± 1	1.3 ± 0.8	370

[a]IC_{50} values for $CuCl_2{\cdot}2H_2O$ and cisplatin are 32 ± 5 and 3.5 ± 0.6 μM, respectively

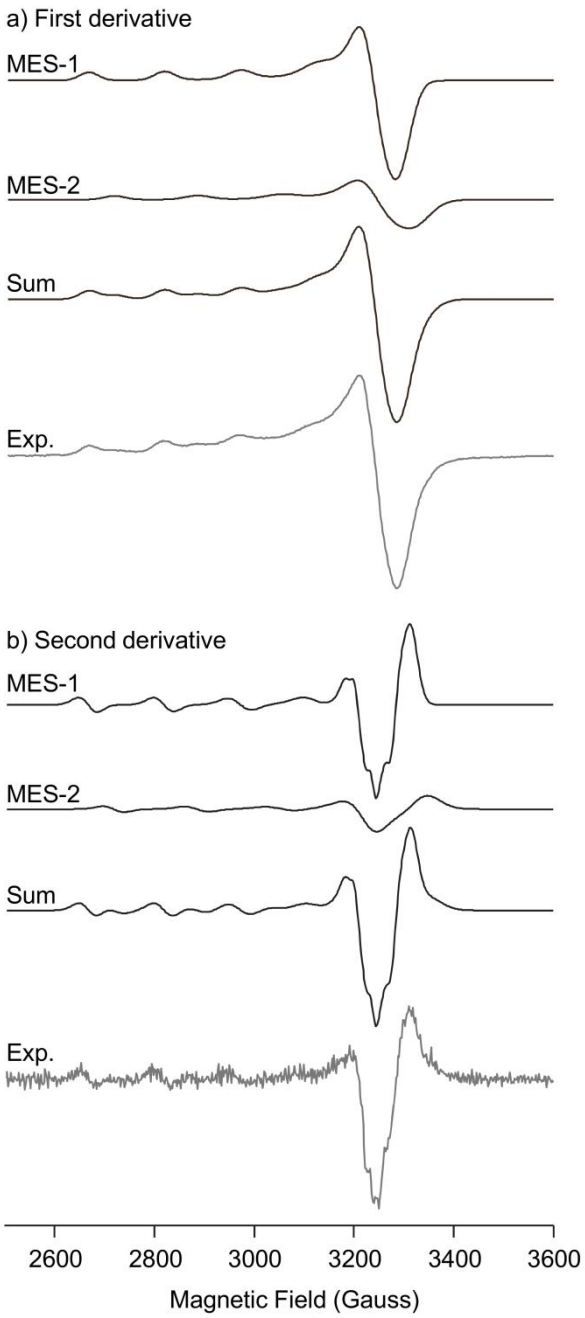

Figure 3. EPR spectrum of Cu(pbzBz) in MES buffer and simulation by deconvolution into two species; a) simulation of first derivative spectrum, b) simulation of second derivative spectrum. Experimental parameters: frequency = 9.38 GHz, microwave power = 2.0 mW, time constant = 40.96 ms, modulation amplitude = 10 G, average of five 1 min scans. For EPR measurements, simulations and deconvolutions of other Cu(pbzX) complexes, see Supporting Information, Figures S17-18. For spectral parameters used in each simulation see Supporting Information, Table S3.

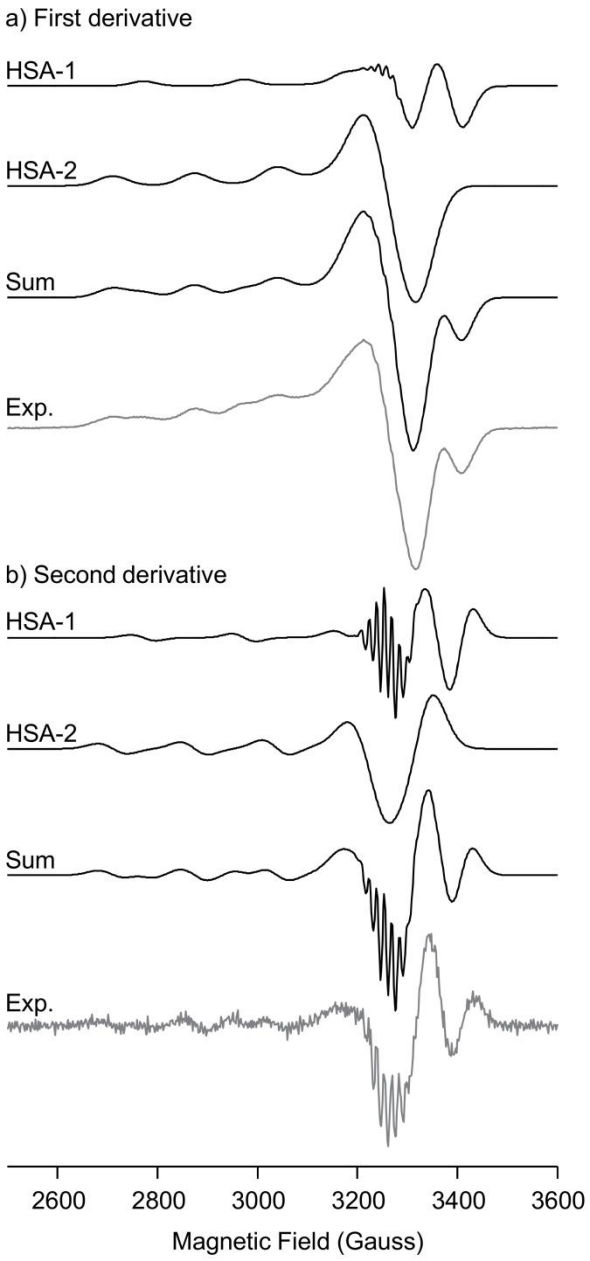

Figure 4. EPR spectrum of Cu(pbzBz) in with HSA and simulation by deconvolution into two species; a) simulation of first derivative spectrum, b) simulation of second derivative spectrum. Experimental parameters: frequency = 9.38 GHz, microwave power = 2.0 mW, time constant = 40.96 ms, modulation amplitude = 10 G, average of five 1 min scans. For EPR measurements, simulations and deconvolutions of other Cu(pbzX) complexes, see Supporting Information, Figures S19-20. For spectral parameters used in each simulation see Supporting Information, Table S4

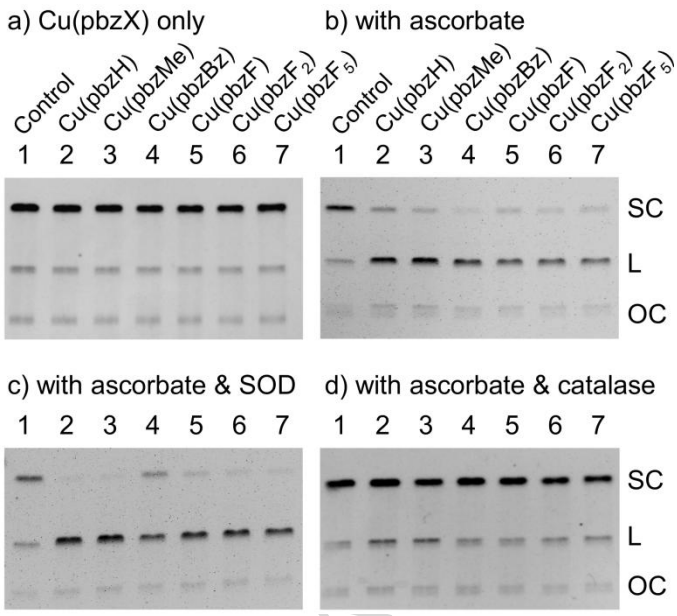

Figure 5. Agarose gel (0.8%) electrophoresis. All lanes contain 10 μM isolated plasmid DNA, which is found in three forms: Supercoiled (SC); Linear (L); Open Circular (OC). Lanes 2-7 contain a copper complex at a concentration of 2 μM. *lane 1*: plasmid with no copper complex; *lane 2*: Cu(pbzH); *lane 3*: Cu(pbzMe); *lane 4*: Cu(pbzBz); *lane 5*: Cu(pbzF); *lane 6*: Cu(pbzF_2); *lane 7*: Cu(pbzF_5). Gel A: Plasmid only; Gel B: *lanes 1-7:* 20 μM ascorbate; Gel C: *lanes 1-7:* 20 μM ascorbate and 1 unit of SOD; Gel D: *lanes 1-7:* 20 μM ascorbate and 1 unit of catalase.

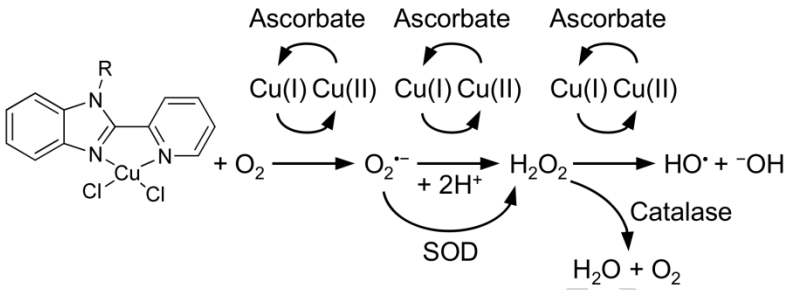

Scheme 2. Generation of reactive oxygen species, as shown by gel electrophoresis of plasmid DNA with Cu(pbzX) and sodium ascorbate.

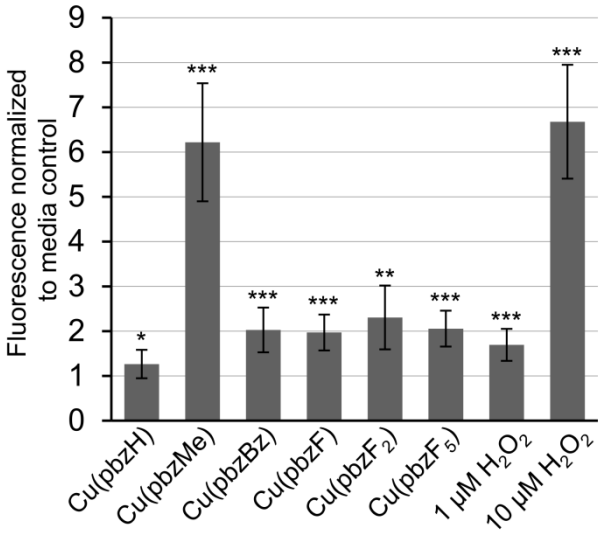

Figure 6. *In vitro* ROS assay of all copper complexes with the A549 cell line. Statistical significance as determined by Student's t test: *** $p<0.001$, ** $p<0.005$, * $p<0.01$ indicating samples are significantly different from the media control.

Anticancer Copper Pyridine Benzimidazole Complexes: ROS Generation, Biomolecule Interactions, and Cytotoxicity

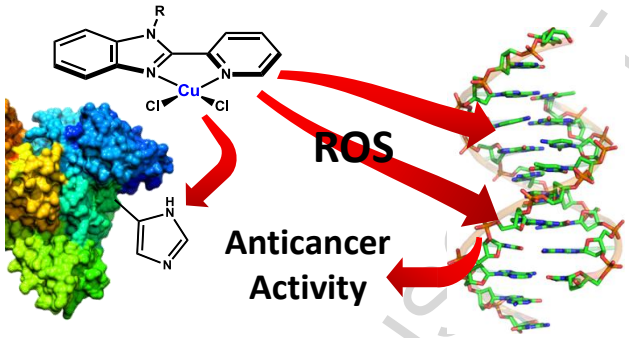

Cytotoxic redox-active copper complexes with functionalized bidentate nitrogen donor ligands and exchangeable chlorides are described. These compounds bind to albumin but interact weakly with DNA. The complexes cleave DNA in the presence of reducing agents and generate reactive oxygen species in cells.

Graphical abstract

Anticancer Copper Pyridine Benzimidazole Complexes: ROS Generation, Biomolecule Interactions, and Cytotoxicity

Kathleen E. Prosser, Stephanie W. Chang, Felix Saraci, Phúc H. Lê, and Charles J. Walsby*

Highlights

1) Synergy between copper centres and ligands generates cytotoxicity.
2) Coordinate and non-coordinate interactions with albumin.
3) Complexes cause DNA cleavage in the presence of ascorbate via hydroxyl radicals.
4) Complexes generate elevated levels of reactive oxygen species in A549 cells.